Karlsruhe Institute of Technology

Institute for Hydromechanics
Kaiserstr. 12
76131 Karlsruhe
www.ifh.kit.edu

Direct simulation of open-channel flow in the fully rough regime : focus on fluid-roughness interaction

Marco Mazzuoli & Markus Uhlmann
marco.mazzuoli@kit.edu, markus.uhlmann@kit.edu

Open-channel flow (OCF) over a rough surface

The interaction of OCF with a rough surface can be observed both in natural and industrial environments and gives rise to different fundamental processes

- It produces the friction head loss and originates the transport of sediments in shallow gravel-bed rivers
- It causes soil erosion of hill slopes and the subsequent formation of grooves
- It is studied for industrial applications to promote the reduction of drag (e.g. flow over riblets)

Short introduction

The turbulence structure in the roughness sublayer and the action of turbulent vortices on the individual roughness elements are presently investigated by means of Direct Numerical Simulation (DNS) of OCF over an array of fixed rigid spheres placed on a flat wall in square arrangement. The values of the fluid and particle Reynolds numbers are in the range at which the flow regime is fully rough. A comparison with the previous work of Chan-Braun et al., JFM (2011), who investigated numerically OCF at the transitionally rough regime in a similar bottom configuration, is also made.

Numerical approach

The approach adopted to numerically solve the incompressible Navier-Stokes equations is based on a second-order fractional-step method. The temporal discretisation is semi-implicit (Crank-Nicolson scheme for the viscous terms and three-step Runge-Kutta procedure for the non-linear part) while spatial operators are evaluated by central finite-differences on a staggered uniform grid. A variant of the immersed boundary method proposed by Uhlmann, JCP (2005) is employed to force the boundary conditions at the sphere surfaces.

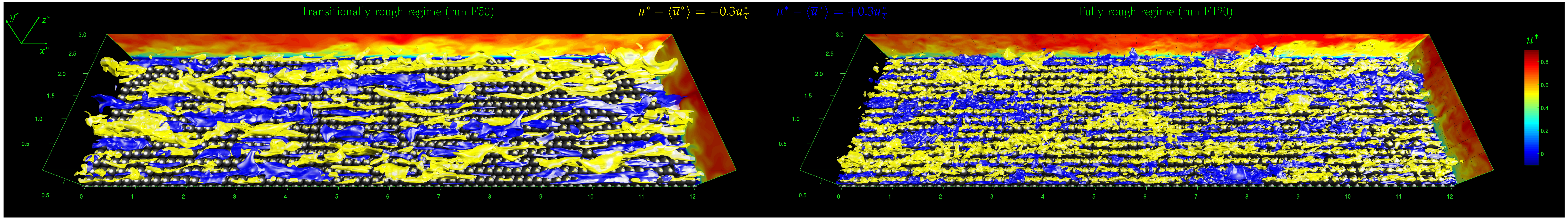

Results: 1.Velocity profiles

line color	run	$\frac{U_{bh}}{u_\tau}$	Re_b	Re_τ	D^+	Δ_x^+	simulation time [bulk units]	N_x	N_y	N_z
red	F10	15.09	2870	190.1	10.87	0.7765	105.0	3072	256	768
blue	F50	12.2	2872	233.7	49.05	1.066	78.0	3072	256	768
black	F120	11.71	6885	578.4	124.8	1.178	88.8	6912	576	1728

- The near-bottom peak of the streamwise velocity root mean square, u'_{rms}, is significantly smoothed and is located beneath the level of sphere crests.
- Velocity fluctuations at the fully rough regime show the tendency to be more isotropic than at the transitionally rough regime

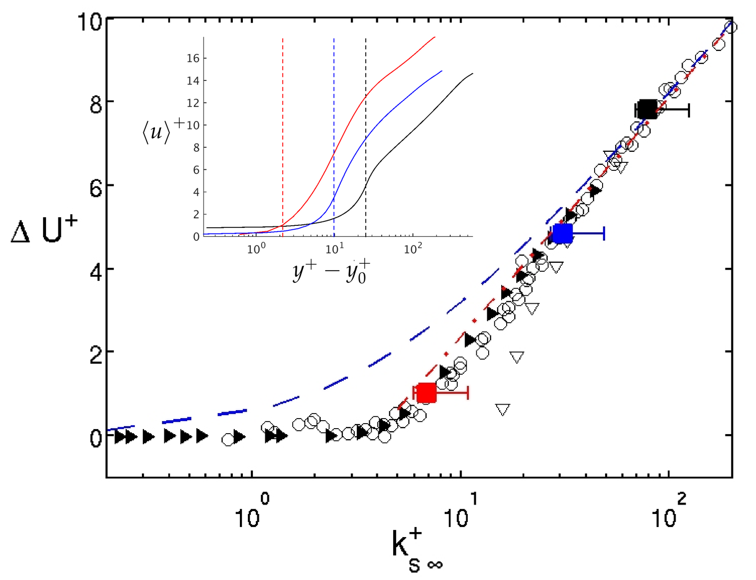

Roughness function as a function of $k^+_{s\infty}$. Nikuradse (1933) (○), Ligrani & Moffat (1986) (▽), Shockling et al. (2006) (▶), present DNS with $k^+_{s\infty} = 0.63D^+$ (■) and error-bars $[0.55, 1]D^+$. Colebrook (1939) (- - -), $\Delta U^+ = 5.75\log(k^+_{s\infty}) - 8.48 + 5.1$ (— · —).

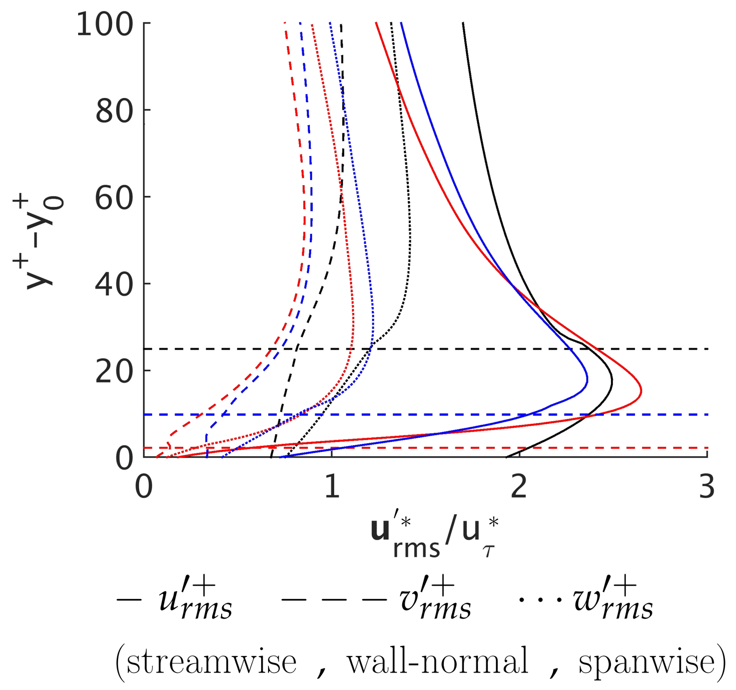

2.Flow structures about the roughness elements

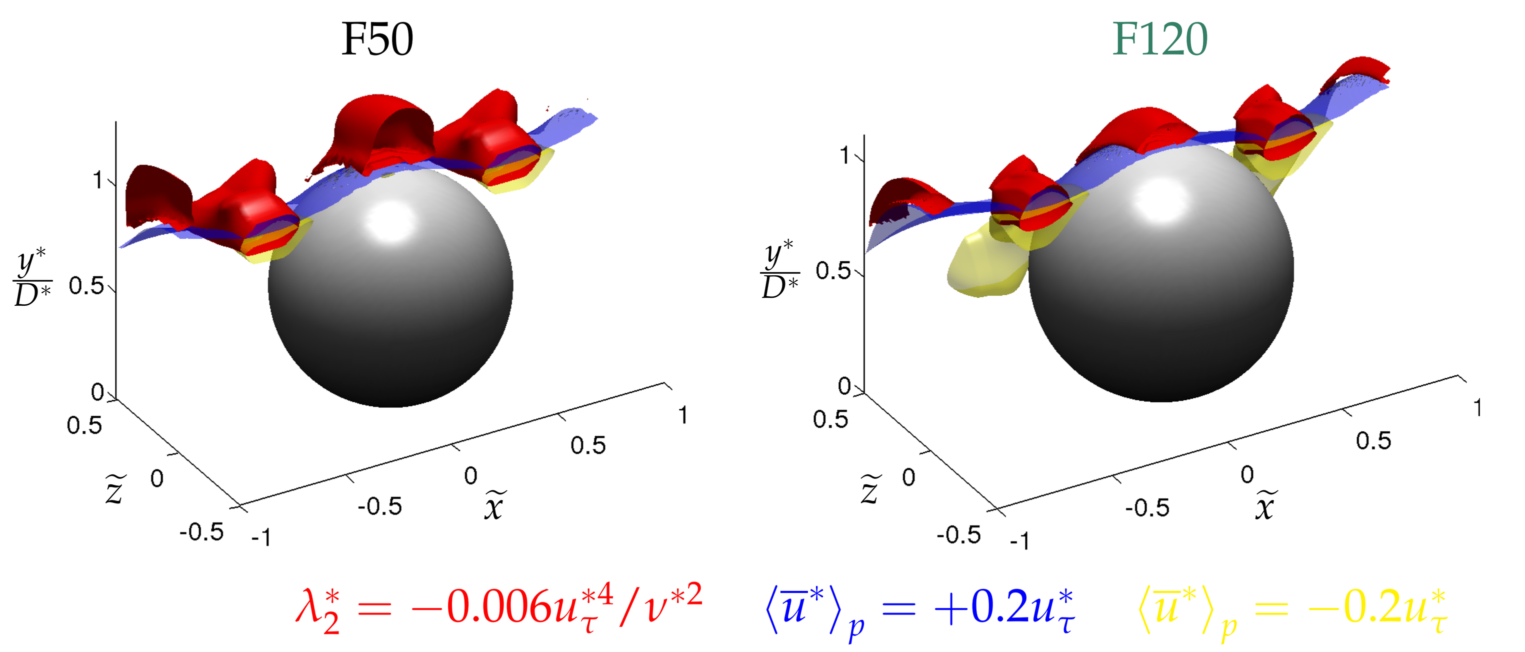

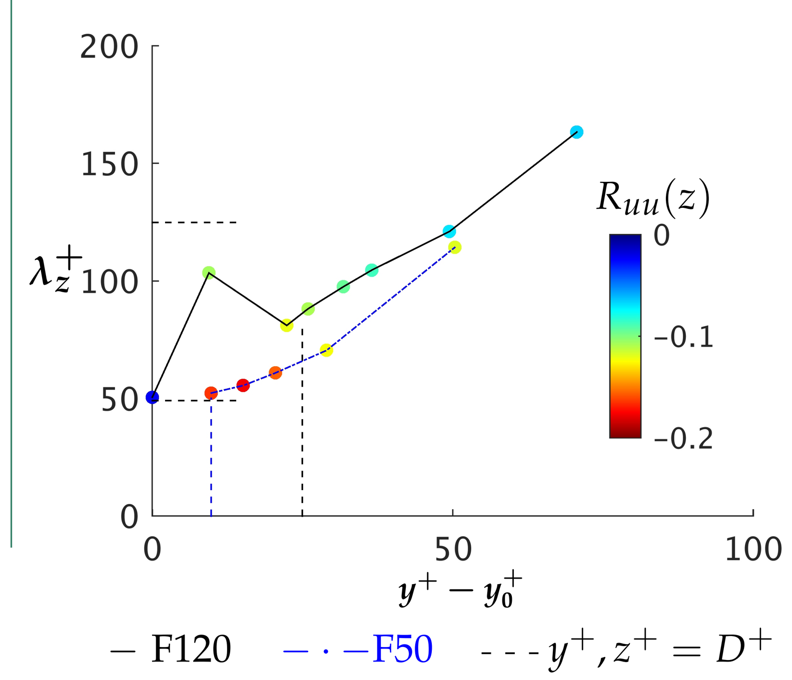

- $\langle\cdot\rangle_p$ and $\overline{(\cdot)}$ denote the spatial-average over particle-periodic boxes and the time-average, respectively
- Flow separates in the horizontal grooves between spheres: the region with negative velocity appears significantly larger in the case F120 than in F50
- Vortices, presently identified by λ_2 isocontours, adhere to the top of the spheres in the case F120, consequently affecting the stress distribution on spheres
- Mean spanwise streaks half-spacing estimated from the two-point correlation: in the case F120, $\lambda_z^+ \sim 80$ which is larger than the typical value observed over a smooth wall $\lambda_z^+ \sim 50$.

3.Hydrodynamic force and torque on spheres

run	$\mathcal{C}_{F_x}$	$\mathcal{C}_{F_y}$	$\mathcal{C}_{F_z}$	α_F	σ_{F_x}/F_R	σ_{F_y}/F_R	σ_{F_z}/F_R	$\mathcal{S}_{F_x}$	$\mathcal{S}_{F_y}$	$\mathcal{S}_{F_z}$	$\mathcal{K}_{F_x}$	$\mathcal{K}_{F_y}$	$\mathcal{K}_{F_z}$
F120	1.13	0.519	0.0065	24.7	1.41	0.772	1.50	0.104	0.317	-0.0354	3.78	4.53	4.55
F50	1.14	0.373	0.0002	18.1	1.31	0.650	1.26	0.0558	0.272	-0.014	5.07	5.76	4.32

Statistics of force on particles. $\mathcal{C}_{F_i} = \langle F_i/F_R \rangle$ denotes the normalized mean force component in the x_i−direction, $\alpha_F = \arctan(\mathcal{C}_{Fy}/\mathcal{C}_{F_x})$ denotes the angle of the resulting force with respect to the x−axis. σ_{F_i}, $\mathcal{S}_{F_i}$ and $\mathcal{K}_{F_i}$ are the standard deviation, the skewness and the kurtosis of the i−th component of the force, respectively.

run	$\mathcal{C}_{T_x}$	$\mathcal{C}_{T_y}$	$\mathcal{C}_{T_z}$	σ_{T_x}/T_R	σ_{T_y}/T_R	σ_{T_z}/T_R	$\mathcal{S}_{T_x}$	$\mathcal{S}_{T_y}$	$\mathcal{S}_{T_z}$	$\mathcal{K}_{T_x}$	$\mathcal{K}_{T_y}$	$\mathcal{K}_{T_z}$
F120	0.0441	-0.0146	-0.460	0.150	0.144	0.131	0.688	0.007	-0.369	4.52	4.59	3.59
F50	-0.0007	-0.0004	-0.722	0.170	0.114	0.273	-0.010	-0.008	-0.747	3.78	4.92	3.35

Statistics of torque on particles. $\mathcal{C}_{T_i} = \langle T_i/T_R \rangle$ denotes the normalized mean torque about x_i. σ_{T_i}, $\mathcal{S}_{T_i}$ and $\mathcal{K}_{T_i}$ are the standard deviation, the skewness and the kurtosis of the i−th component of the torque, respectively.

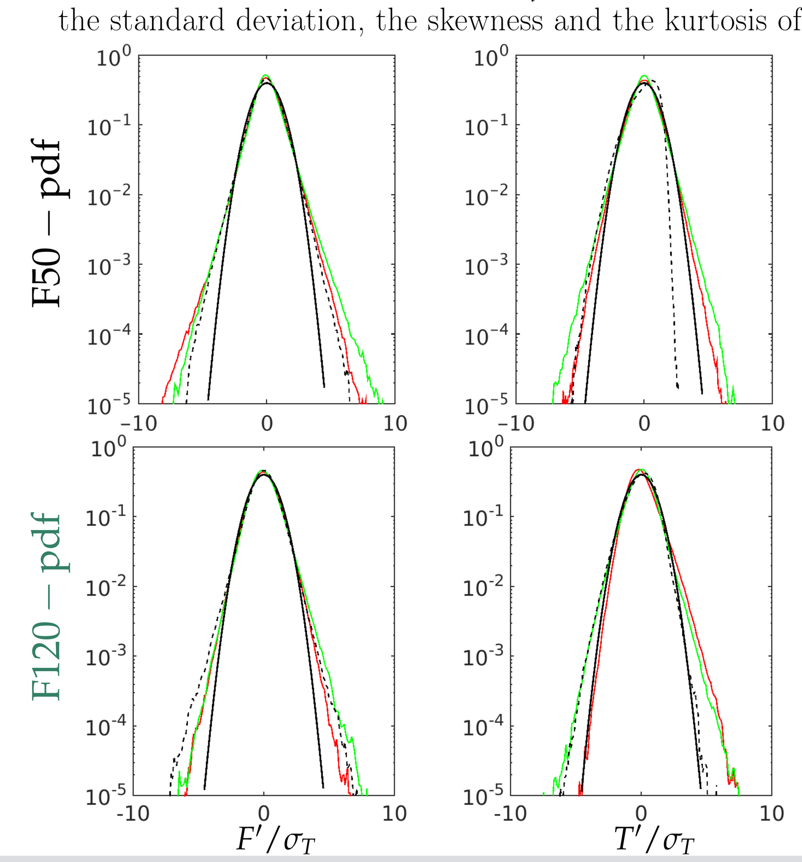

- Lift remarkably increases with increasing Reynolds number. This possibly enhances the capability of the flow to dislodge particles from their pocket at the fully rough regime
- Both the value of kurtosis $\mathcal{K}_{F_i}$ and $\mathcal{K}_{T_i}$ related to force and torque instantaneously acting on spheres approaches 3 (in particular case F120) similarly to Gaussian distribution of probability
- Positive fluctuations of lift are stronger than negative fluctuations both in case F50 and F120
- The reduction of spanwise torque in case F120 is balanced by streamwise and wall-normal torque (flow is more isotropic)